







Article

Manufacturing of PAV-ONE, a Permeator against Vacuum Mock-Up with Niobium Membrane

Francesca Papa ¹, Alessandro Venturini ^{2,*}, Gianfranco Caruso ¹, Serena Bassini ², Chiara Ciantelli ²,
Angela Fiore ², Vincenzo Cuzzola ², Antonio Denti ³ and Marco Utili ²

¹ DIAEE Department, Sapienza University of Rome, 00186 Rome, Italy

² ENEA, Italian National Agency for New Technologies Energy and Sustainable Economic Development, Fusion and Technology for Nuclear Safety and Security Department, Brasimone Research Centre, Camugnano, 40032 Bologna, Italy

³ RINA Consulting—CSM S.p.A., 00128 Rome, Italy

* Correspondence: alessandro.venturini@enea.it

Abstract: The Permeator Against Vacuum (PAV) is one of the proposed technologies for the Tritium Extraction System of the WCLL BB (Water-Cooled Lithium-Lead Breeding Blanket) of the EU DEMO reactor. In this paper, the manufacturing of the first PAV mock-up with a niobium membrane with a cylindrical configuration is presented. This work aimed to demonstrate the possibility of manufacturing a relevant-size PAV to be later tested in the TRIEX-II facility. The adopted prototypical solutions are described in detail, starting with the methodology developed to join the Nb tubes with a 10CrMo9-10 (A182 F22) plate. Dedicated manufacturing and welding procedures, based on vacuum brazing with a nickel-based brazing alloy, were developed to solve the problem. This new kind of brazing was first analyzed to check the morphology of the joint and then tested to check its capability to withstand the TRIEX-II operative conditions. In parallel, the compatibility with a lithium-lead environment was analyzed by exposing samples of niobium and 10CrMo9-10 (A335 P22) to a flow of the eutectic alloy at 500 °C up to 4000 h. Finally, the PAV mock-up was installed in the TRIEX-II facility.

Keywords: Permeator Against Vacuum; tritium extraction; niobium membrane



Citation: Papa, F.; Venturini, A.; Caruso, G.; Bassini, S.; Ciantelli, C.; Fiore, A.; Cuzzola, V.; Denti, A.; Utili, M. Manufacturing of PAV-ONE, a Permeator against Vacuum Mock-Up with Niobium Membrane. *Energies* **2023**, *16*, 5471. <https://doi.org/10.3390/en16145471>

Academic Editor: Gediminas Stankūnas

Received: 30 April 2023

Revised: 13 June 2023

Accepted: 27 June 2023

Published: 19 July 2023



Copyright: © 2023 by the authors. Licensee MDPI, Basel, Switzerland. This article is an open access article distributed under the terms and conditions of the Creative Commons Attribution (CC BY) license (<https://creativecommons.org/licenses/by/4.0/>).

1. Introduction

The Permeator Against Vacuum (PAV) is considered one of the most promising technologies for the Tritium Extraction and Removal System [1] of the WCLL BB (Water-Cooled Lithium-Lead Breeding Blanket) [2] of the EU DEMO fusion reactor, together with the Gas–Liquid Contactor. It is a compact component that can directly remove tritium from the LiPb, and it has high theoretical efficiency. The PAV technologies work with a concentration gradient between two sides of a membrane, with one side in contact with LiPb, which carries tritium, and the other one where vacuum is pumped [3]. The selected membrane material needs to have high tritium permeability, such as α -iron [4], vanadium or niobium [5]. CIEMAT and Idaho National Laboratory are working on a vanadium membrane in a rectangular channel (TRITON) [6] and modular tubular (TEX) configuration [7]. Instead, niobium membranes in a tubular configuration are under investigation at ENEA Brasimone Research Centre.

However, a PAV mock-up has never been manufactured and tested at relevant operative conditions, mainly due to the manufacturing issues linked to the materials that are necessary to use for the proper operation of the technology. Indeed, both niobium and vanadium have much higher melting temperatures than steels, meaning that the welding is not possible. Other joining techniques have been tested, but they failed to guarantee the necessary vacuum requirements on the low-pressure side of the permeable membrane. In

order to cover this technologic gap, a dedicated brazing technology has been developed and is described in this paper.

This paper describes the first PAV mock-up, named PAV-ONE, to ever be successfully built with relevant dimensions, whose engineering design is described in [8]. The work has been performed by ENEA Brasimone in collaboration with RINA C.S.M. and Sapienza University of Rome. The PAV-ONE mock-up adopts niobium as the membrane material, 316 stainless steel as the structural material for the vacuum side and F22 ferritic steel (10CrMo9-10) as the structural material for the other parts in direct contact with LiPb. The most important challenge faced during the manufacturing was joining the F22 plate and the niobium pipes. An important aspect that was also investigated is the compatibility of niobium with flowing LiPb, tested in an experimental campaign in IELLLO facility [9], devoted to characterizing relevant materials for the WCLL BB in flowing LiPb. The manufactured mock-up is the subject of a testing campaign in the TRIEX-II facility [10] at ENEA Brasimone Research Centre [11], which will characterize the performances of the PAV technology at relevant operative conditions and shed new light on the possibility to use it as a tritium extraction system in a fusion reactor. The experiments in flowing LiPb foresee ranges of temperature (350–450 °C) and hydrogen partial pressure (100–300 Pa) relevant for the current configuration of the WCLL TER [12].

2. The Manufacturing

2.1. Brief Description of the Mock-Up

The manufactured PAV mock-up follows the conceptual and engineering design carried out by ENEA, Sapienza University of Rome and Politecnico di Torino. The design activities are described in detail in [8].

It has a shell and tube configuration, with 16 niobium U-pipes (inner diameter of 9.2 mm and total length of about 2 m) joined with an F22 plate, which is the structural material of the whole TRIEX-II facility. This ferritic steel was selected due to its high corrosion resistance to flowing LiPb compared to stainless steels. Besides the obvious advantage of the increased piping resistance, the choice of F22 was motivated by the reduced amount of corrosion products that would contaminate LiPb, introducing additional uncertainties in the analysis of the experimental results.

The niobium pipes were inserted in a vacuum chamber which was installed above a LiPb collector that served as a distributor for the liquid metal, allowing it to be spread among the pipes. LiPb flowed in two passages in the internal part of the U-pipes. In order to achieve this, the collector was divided into three sectors: LiPb coming from the facility entered the first eight pipes from the first sector and merged again in the second sector before entering the second group of eight pipes, and finally exited the mock-up, passing through the final sector (Figure 1). During its path, LiPb was heated by four infrared (IR) lamps that avoided its solidification, maintaining the required test temperature.

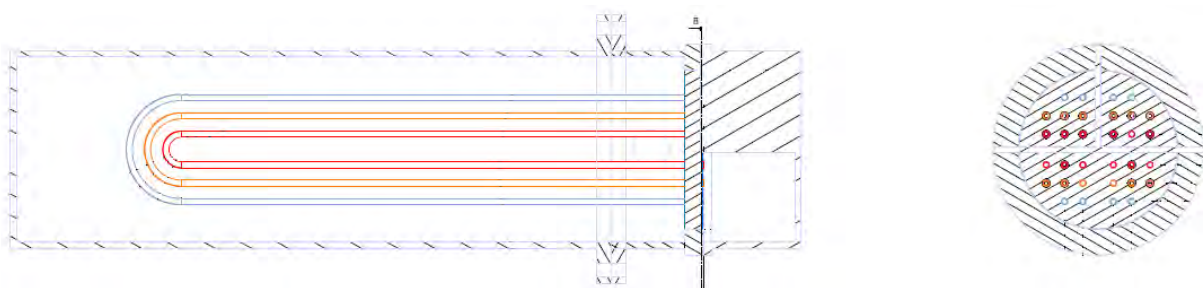


Figure 1. Drawings of the PAV-ONE mock-up: on the left, the axial cross-section with three U-pipes with different curvature radii; on the right, a cross-section of the tube plate divided in three sectors to allow the LiPb to spread into the tubes.

During the tests, the vacuum chamber was constantly maintained under vacuum conditions to allow hydrogen extraction from the alloy. The vacuum was pumped below 1 Pa using a leak detector ASM340 series supplied by Pfeiffer Vacuum (Aszlar, Germany) that also had the task of measuring the hydrogen flux that permeated through the niobium pipes. The instrument had an integrated vacuum station and a mass spectrometer tuned to measure only hydrogen or helium, following the inputs by the operators.

2.2. Manufacturing of the Tube Bundle

Joining the niobium tubes to the F22 structure has been one of the most innovative challenges in the manufacturing of PAV-ONE. Three issues had to be faced:

- Niobium has a tendency to oxidize, especially at high temperature;
- Using a welding procedure had to be ruled out because of the difference in the melting temperature of niobium and F22 steel (2469 vs about 1350 °C);
- LiPb easily dissolves most of the materials used to perform brazing (e.g., nickel).

Therefore, the solution that was found to perform this joining was to carry out a brazing under vacuum, thus preventing niobium to get oxidized, while keeping the brazing material (also based on nickel) away from LiPb. To do this, an annular pocket was created between the niobium tube and the plate and filled with the brazing alloy. The choice of the nickel-based alloy was motivated by its resistance to high temperatures, much higher than the operative ones (about 450 °C).

Every brazing was checked by radiography after the experimental campaign. However, a sample was prepared to be tested with destructive methods before launching the manufacturing of the entire mock-up. This was motivated by innovative nature of the adopted manufacturing solution.

Given the prototypical nature of this technique, sample joints were realized with the specific purpose of testing their resistance and the overall quality of the postulated solution. Visual examination and pressure tests were performed on some samples to check that the joints were well made. Tests were carried out with high pressures up to 24 bar at 25 °C with helium (24 bar is the equivalent pressure at room temperature of 1 bar and 480 °C, according to the Pressure Equipment Directive 2014/68/EU [13]). These tests were repeated with three different samples. All three samples withstood this pressure. Moreover, a visual examination of all the welded pipes was made, and all the joints met the requirements of international standards, such as ISO 18279 [14]. Figure 2 shows a detailed view of the stereoscope analysis, the pressure test device and two samples of the Nb pipe joined with the F22 plate.

A metallographic investigation with Scanning Electron Microscopy (SEM) was carried out by RINA c.s.m. on two cross-sections of two different samples (Figure 3). The metallographic analyses showed that the brazing alloy had a good pocket between the plate and each pipe and excellent penetration, with a total thickness of about 130 µm. Moreover, the analyses showed structural cohesion of about 12 microns between the brazing alloy and the walls of the tube and of the flange, as shown in Figure 3c. These cohesion layers were formed via the mutual diffusion of atoms of the base material into the brazing alloy and vice versa. High-quality cohesion leads to better mechanical performances.

In addition, the metallographic analysis revealed isolated micro porosities in the middle of the brazed section. The largest size of the porosity found during the SEM analyses of the first brazing samples did not exceed 0.16 mm. If we consider the brazing area in the section (about 1 square millimeter), the presence of these defects only affected 1.5% of the cross-section. Therefore, it is considered that this type of isolated defect did not affect the overall performance of the joint. With reference to ISO 18279 level B, the limit of acceptable porosity is 20% of the projected area.



Figure 2. Examination and testing of the joining solution. From the top: detail of the stereoscope analysis; picture of two pressure test samples; pressure test device.

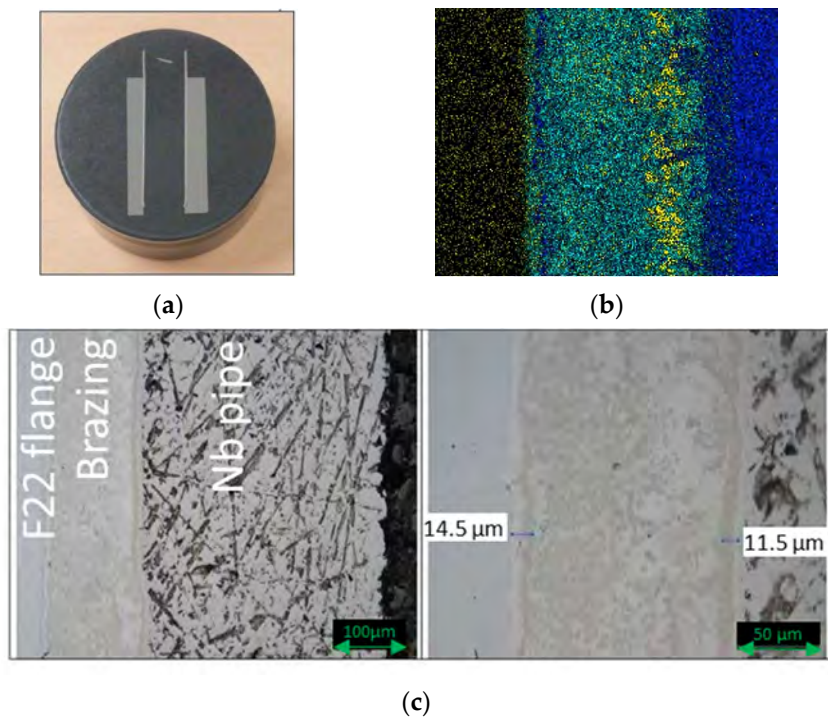


Figure 3. Cont.

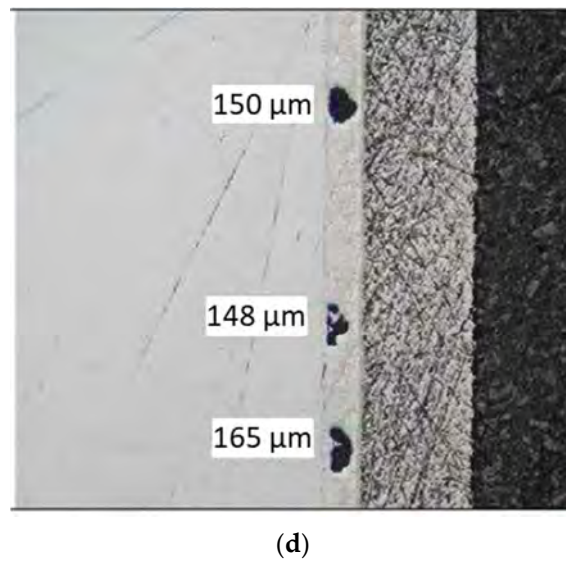


Figure 3. SEM analysis of the Nb-F22 joint. From the top: (a) picture of a section analyzed via SEM; (b) composition of the joint; (c) small porosities in the joint; (d) details of some defects in the observed joint.

2.3. Shaping the Nb Pipes

Niobium showed high ductility, and it was not difficult to shape the channels using a bending jig and filling the pipes with sand. The bending process had to be slow and continuous to avoid the deformation of the pipe's internal side in contact with the jig. Furthermore, duct tape was utilized to protect the contact zone between the pipe and the bending jig during the hand bending. Figure 4 shows the U-shape pipes joined with the F22 plate.

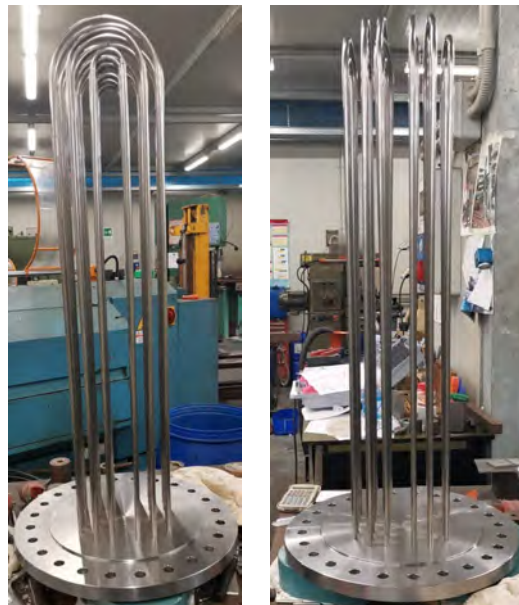


Figure 4. Pictures of the 16 U-shaped niobium pipes after brazing with the F22 flange.

2.4. Instrumentation and Connections with TRIEX-II Facility

A total of 60 thermocouples and four infrared lamps were installed inside the vacuum chamber of the PAV mock-up. Two thermocouples were installed on each pipe close to the LiPb inlet and outlet sections, one more for each pipe on the top of the U, while the last twelve thermocouples were positioned at the half height of some selected pipes, trying to

take advantage of the symmetries of the bundle to achieve the most accurate temperature mapping. The control system of the facility would monitor all the thermocouples and would control the infrared lamps so that the minimum temperature in each location was above a threshold selected by the operators.

Figure 5 shows the solution adopted to allow the installation of the instrumentation without affecting the vacuum quality. Six stainless steel feedthroughs by Vaqtec were installed on two nozzles to bring the thermocouple signals outside of the vacuum chamber, while eight power feedthroughs were welded onto two different nozzles to power the infrared lamps (one nozzle of each type is hidden behind the mock-up vessel in the figure).

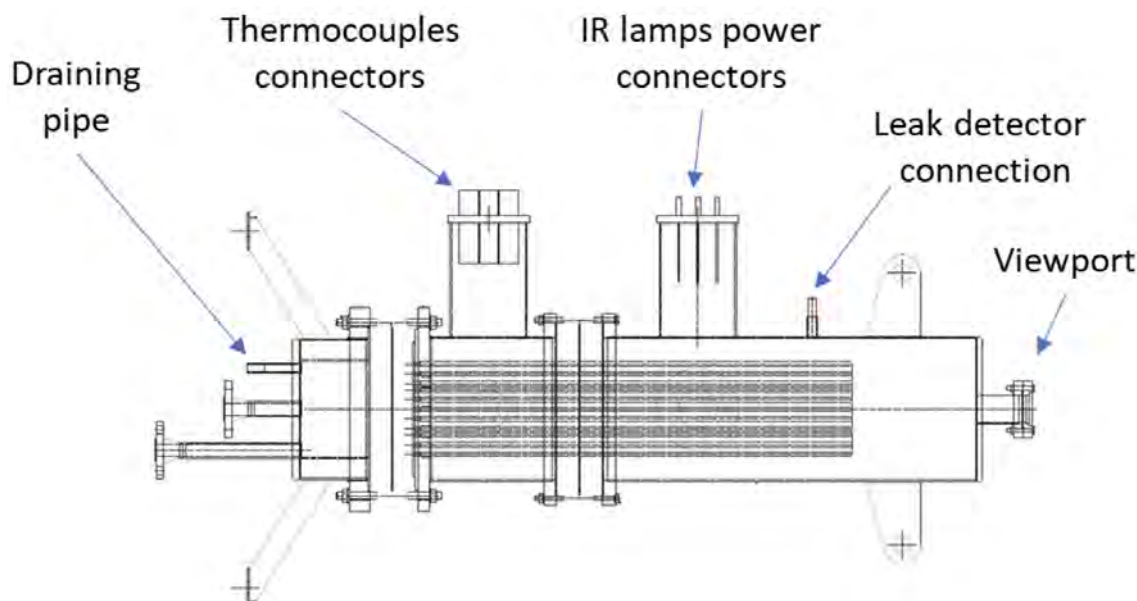


Figure 5. Final technical drawing of the mock-up.

The leak detector was connected to a $\frac{1}{2}$ " Swagelok pipe welded to the upper part of the vessel by means of a flexible hose.

A viewport was installed on the top of the vessel to have vision of the niobium pipes during operation. A camera was installed above the viewport to allow the operators to monitor the vessel directly from the control room.

On the left of Figure 5, it is possible to distinguish the two pipes that connected the mock-up to TRIEX-II facility and the one used to drain the intermediate sector of the collector. The latter was connected to a valve that was kept closed during operation, but it was necessary to allow the discharge at the end of the experiments.

3. Niobium Compatibility with LiPb

The low solubility of niobium in LiPb was found by Feuerstein et al. [15] and Grabner et al. [16] by exposing niobium samples to stagnant LiPb. However, also characterizing the niobium compatibility with flowing LiPb was deemed fundamental before starting the manufacturing of the PAV mock-up, and from a wider perspective, to allow the use of this material in LiPb systems. For this reason, an experimental campaign was conducted in the IELLLO facility [17]. IELLLO uses eutectic LiPb as the working fluid (15.7% at. Li) and pure argon (99.999%) as the cover gas during operation and filling gas when the facility is not in operation. Niobium samples, together with other main materials relevant for the WCLL BB, were exposed to high-temperature flowing LiPb, with a speed of 0.5 m/s, the maximum one foreseen in the WCLL TER, and a temperature of 500 °C. This temperature was chosen to be conservative with respect to the temperatures expected in the Tritium Extraction Unit of the WCLL TER.

The test section where the specimens were placed was composed of three 1" pipes, and each of these pipes accommodated a rod of specimens. Niobium bars with a nominal purity of 99.9% wt. were supplied by Goodfellow (Lille, France). The samples were tested for 1000, 2000 and 4000 h to characterize the increasing effect of corrosion with time. A total of 12 niobium samples were exposed, and 4 of them were removed from the test section at each exposure time.

Various characterization techniques were used to analyze the samples at ENEA Brasimone, including an FEI QUANTA INSPECT Scanning Electron Microscope (SEM) equipped with an EDAX Energy Dispersive X-Ray (EDX) microanalysis and X-ray diffraction (XRD), utilizing a PHILIPS X'Pert Pro diffractometer. SEM analysis provided information about the morphology and surface geometry of the samples, while EDX analysis offered insights into the chemical composition, the distribution and the concentration of elements present in the samples. XRD was used to identify potential crystalline compounds formed on the surface of the samples. Moreover, the samples were weighted before and after the exposure to quantify the material loss at different exposure times.

The weighting of the samples indicated a very slight and not significant increase in weight with the exposure times, ascribable to the presence of small LiPb traces likely having remained attached to the samples, despite the cleaning procedure performed before the weighting, especially to the threaded head that was used to connect the specimens. Moreover, the detailed characterization of the samples showed that chemical compounds of iron and nickel with niobium were formed on the sample surfaces, and this probably had an impact on the increasing sample weight. After 4,000 h of exposure, however, the weight gain of the samples was very low and measured to be about $+4.0 \text{ g/m}^2$, which corresponded to an increase in thickness of about $0.5 \text{ }\mu\text{m}$, indicating that niobium samples are considerably resistant in LiPb at the given operational conditions.

Considering the detailed analysis, the niobium specimens exhibited an increasing surface roughness with time, as shown via the SEM analyses in the cross-section (Figures 6–8).

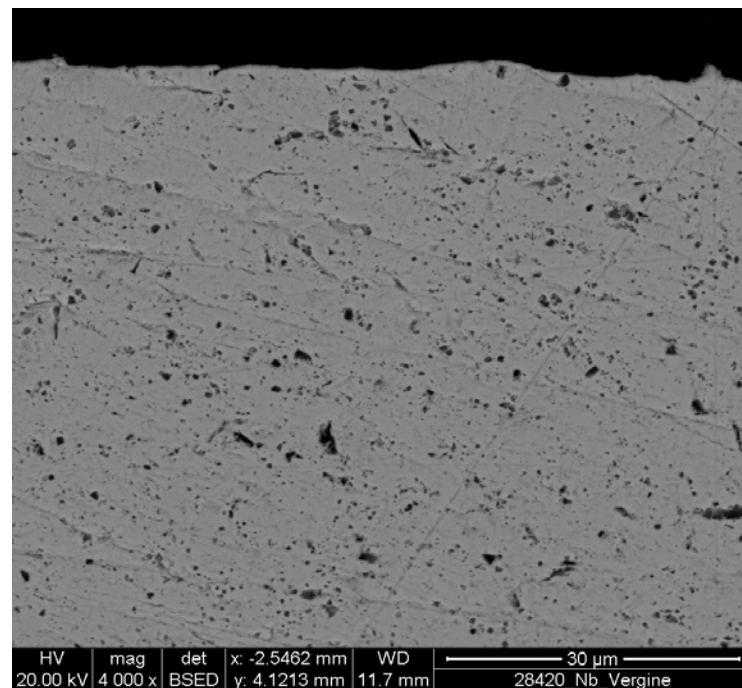
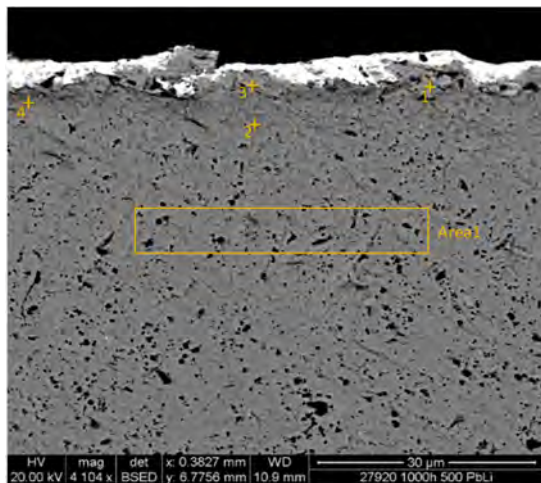


Figure 6. Cross-section SEM image $4000\times$ of a virgin Nb sample.



Element		NbL	PbL	FeK	NiK
Area 1	Wt%	100	/	/	/
	At%	100	/	/	/
Spot 1	Wt%	100	/	/	/
	At%	100	/	/	/
Spot 2	Wt%	100	/	/	/
	At%	100	/	/	/
Spot 3	Wt%	89.1	8.1	1.9	0.8
	At%	91.6	3.7	3.3	1.3
Spot 4	Wt%	100	/	/	/
	At%	100	/	/	/

Figure 7. Cross-section SEM image 4000× and composition analysis via EDX of uncleaned Nb sample after 1000 h.

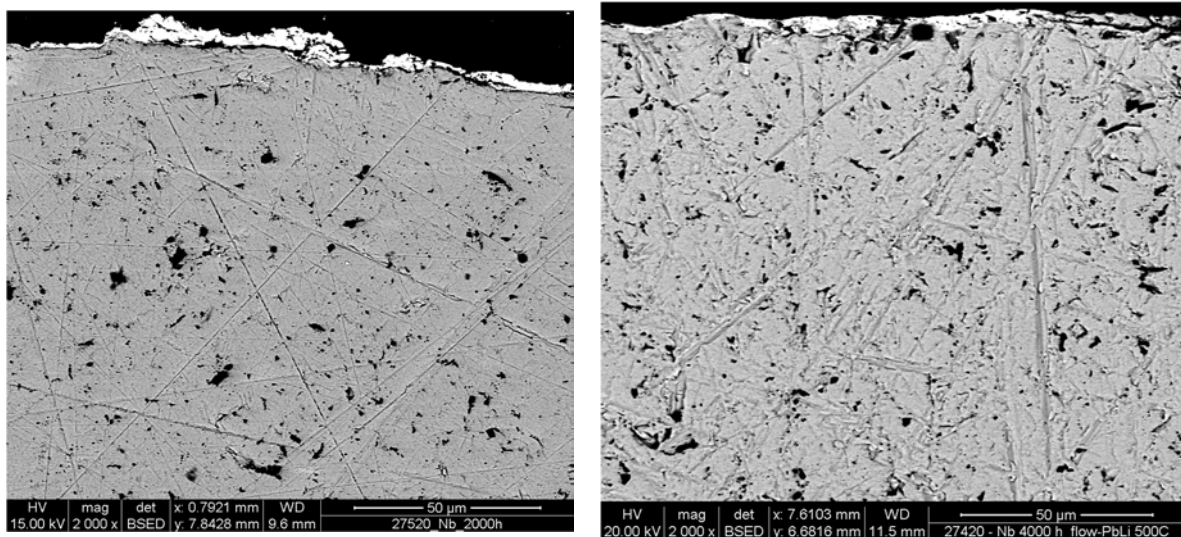


Figure 8. Cross-section SEM images 2000× of Nb samples after 2000 h (left) and 4000 h (right).

Based on the chemical composition analysis, it was observed that there were no major changes in the sample at the interface. However, after 1000 h, small amounts of Ni and Fe were detected on the surface of the sample, as well as within the LiPb, that adhered to the surface, as shown in Figure 7. These impurities, found also in samples exposed for 2000 h and 4000 h, are suspected to have originated from the corrosion products found in the LiPb, which may have come from the corroded piping of the loop. Figure 8 also gives a visual representation of the surface cross-section and the rugosity after 2000 h and 4000 h. Figure 7 provides a visual representation of this contamination.

Moreover, the performed surface SEM examinations, shown in Figure 9 for 2000 h, confirm the enrichment in Ni and Fe. Samples exposed for 1000 and 4000 h depicted a similar picture. It is not possible to draw a definite conclusion about this point based only on the SEM-EDX analysis. Nonetheless, the presence of a considerable quantity of O on the surface could potentially suggest the development of a combination of NbFeNi-oxide. Additionally, XRD analysis may aid in determining whether any mixed-oxide compounds had indeed been formed.



Element	OK	NbL	PbM	FeK	NiK	
Spot 1	Wt%	12.74	06.15	78.75	/	02.36
	At%	62.08	05.16	29.63	/	03.13
Area 2	Wt%	19.36	61.57	/	03.12	15.95
	At%	55.00	30.12	/	02.54	12.35

Figure 9. Longitudinal SEM image and elemental composition via EDX of uncleaned Nb sample after 2000 h.

Therefore, XRD spectra were obtained from the exposed specimens to identify possible compounds, which showed the dominant phase in the 2000 h specimen was Nb, while the Nb₃Ni phase was stabilized by the higher Ni content in the specimens exposed for 4000 h (shown here in Figure 10). These findings are in agreement with the ternary-phase diagram section at 500 °C [18] but do not indicate the presence of specific oxides available in the XRD database. The findings then suggest that the presence of oxygen shown in the previous surface examination may be related to other oxidation effects, for example, occurring during draining in hot argon before extraction, or related to the formation of stable mixed oxides not identified in XRD databases or those that are too thin in thickness to be detected using XRD analysis.

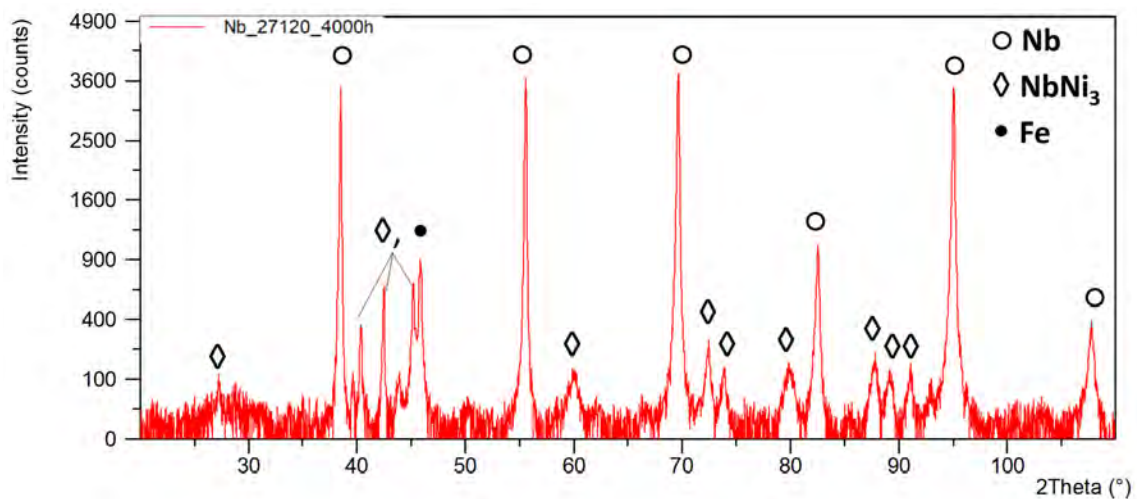


Figure 10. XRD pattern for Nb samples exposed for 4000 h.

4. Non-Destructive Testing

The connections between the niobium pipe and support plates are critical during the manufacturing of the PAV for the WCLL BB of the EU DEMO reactor. To ensure the infrastructure is maintained correctly and to prevent accidents, it is essential to examine these connections through non-destructive testing (NDT) techniques. NDT allows inspectors to gather information about a material or component without causing any permanent modifications to it.

The failure of connections can occur due to inadequate adherence to welding and brazing specifications, such as welding temperature, cooling rate and compatible materi-

als. Moreover, there are various welding/brazing defects that could cause a joint to fail, including a lack of fusion, cracks or porosity inside the welding/brazing and variations in welding/brazing density. In the preliminary assessment of the better technique to detect these defects in PAV components, the study focused on both the volumetric and superficial NDT methodologies. The former highlighted defects in the entire volume of the component, while the latter only showed defects on or near the surfaces. Therefore, the techniques useful for PAV application are the volumetric ones, such as Ultrasonic NDT, Radiography NDT, Acoustic Emission NDT and Infrared and thermal NDT. However, a visual inspection is suggested before the volumetric one to verify that the joint geometry is compliant with the design constraints.

From the group of volumetric methodologies, transmission and reflection methods were analyzed. In particular, radiography NDT is a transmission method in which the rays pass through all the material to be detected on the other side by a sensor. Ultrasonic NDT, on the other hand, is a reflection method, but it can also be used in a transmission way. Acoustic emission and infrared and thermal NDT are based on energy emissions by the material and are classified separately. While transmission methods have the advantage of low attenuation of the signal, they require an accessible material on both sides of the sample, which was not possible in the PAV application.

Currently, the most common kind of NDT used in the inspection of components having a shell and tube heat exchanger design is ultrasonic NDT. In this process, high-frequency sound waves are transmitted into a material to find variations in the properties. Pulse echo is a common technique used to perform ultrasonic testing and consists of measuring the echoes coming from imperfections towards the receiver.

So, the method proposed for the PAV application was Multigroup Phased Array Ultrasonic Testing (PAUT). In these instruments, many rectangular crystals are placed in a row and they emit ultrasonic waves. These waves travel into the material and, only in the presence of defects, are reflected back to the sensors. The advantage of this technique is that the use of several crystals allows a very accurate analysis and a fast inspection speed.

The main challenges faced in the PAV application would be the small diameter of the niobium pipes, the tight arrangement of the tube bundle and the small size of the defects to be detected. A preliminary investigation conducted with different suppliers showed the feasibility of the development of dedicated probes.

5. Discussion and Conclusions

Starting from an engineering design developed by ENEA Brasimone in collaboration with Sapienza University of Rome and Politecnico di Torino, the manufacturing of the PAV-ONE mock-up was completed, and the mock-up was installed in the TRIEX-II facility, as shown in Figure 11, followed by a set of commissioning tests including leak tests for the vacuum side and tightness tests for the LiPb side. Figure 12 shows a picture of the mock-up interior during the first heating process with the infrared lamps. The success of this work will allow the first characterization of the PAV technology to be performed, which will give insights into the possibility to use it as a tritium extraction system for fusion reactors adopting LiPb as the breeder material.

As far as the manufacturing is concerned, the most innovative result of this work is the solution adopted to join the niobium pipe with the F22 plate. The idea, developed together with experts from RINA C.S.M., was to use vacuum brazing based on a nickel-based brazing alloy (capable of withstanding up to 1100 °C). Vacuum brazing avoids the oxidation of niobium, while, to prevent nickel from solubilizing in LiPb, the brazings were carried out in such a way that avoided contact between the filler material and the LiPb. The brazing was performed on almost the entire depth of the plate in order to create a strong joint between the two materials. Each brazing was later inspected with non-destructive testing (radiography) and checked for potential leakages with helium.



Figure 11. Pictures of PAV-ONE mock-up and its installation in the TRIEX-II facility.



Figure 12. Picture of the niobium pipes heated by the infrared lamps from the viewport installed on the top of the PAV-ONE vessel.

Before exposing the mock-up to flowing LiPb, the compatibility of niobium with the alloy was characterized in the IELLLO facility by exposing samples to flowing conditions at 500 °C for 4000 h. The samples did not show relevant signs of corrosion, even though the performed analyses showed the tendency of niobium to form compounds with nickel. Nickel was likely brought into contact with the niobium samples after the corrosion of the stainless steel piping in the IELLLO facility. However, in the WCLL TER, LiPb will be continuously purified from corrosion products via the action of the cold traps and, therefore, the nickel compounds should not be relevant for the PAV in DEMO. Therefore, this activity allows us to conclude that niobium has good compatibility with LiPb and can be safely used as membrane material in a PAV system.

Author Contributions: Conceptualization, M.U. and F.P.; methodology, A.V. and M.U.; formal analysis, F.P. and A.V.; investigation, A.F., C.C., S.B., A.D., V.C. and F.P.; resources, M.U. and G.C.; data curation, A.V. and F.P.; writing—original draft preparation, F.P.; writing—review and editing, A.V., M.U., S.B. and C.C.; visualization, F.P.; supervision, G.C. and M.U.; project administration, M.U.; funding acquisition, M.U. All authors have read and agreed to the published version of the manuscript.

Funding: This work has received funding from the European Union via the Euratom Research and Training Programme (Grant Agreement No 101052200).

Data Availability Statement: The data presented in this study are available on request from the corresponding author.

Acknowledgments: This work has been carried out within the framework of the EUROfusion Consortium, funded by the European Union via the Euratom Research and Training Programme (Grant Agreement No 101052200). The views and opinions expressed are, however, those of the author(s) only and do not necessarily reflect those of the European Union or the European Commission. Neither the European Union nor the European Commission can be held responsible for them. The work of A. Venturini was financially supported by a EUROfusion Engineering Grant.

Conflicts of Interest: The authors declare no conflict of interest.

References

1. Mozzillo, R.; Utili, M.; Venturini, A.; Tincani, A.; Gliss, C. Integration of LiPb loops for WCLL BB of European DEMO. *Fusion Eng. Des.* **2021**, *167*, 112379. [[CrossRef](#)]
2. Del Nevo, A.; Arena, P.; Caruso, G.; Chiovaro, P.; Di Maio, P.; Eboli, M.; Edemetti, F.; Forgione, N.; Forte, R.; Froio, A.; et al. Recent progress in developing a feasible and integrated conceptual design of the WCLL BB in EUROfusion project. *Fusion Eng. Des.* **2019**, *146*, 1805–1809. [[CrossRef](#)]
3. Bonifetto, R.; Utili, M.; Valerio, D.; Zanino, R. Conceptual design of a PAV-based tritium extractor for the WCLL breeding blanket of the EU DEMO: Effects of surface-limited vs. diffusion-limited modeling. *Fusion Eng. Des.* **2021**, *167*, 112363. [[CrossRef](#)]
4. Tahara, A.; Hayashi, Y. Measurements of Permeation of Hydrogen Isotopes through α -Iron by Pressure Modulation and Ion Bombarding. *Trans. Jpn. Inst. Met.* **1985**, *26*, 869–875. [[CrossRef](#)]
5. Malo, M.; Garcinuño, B.; Rapisarda, D. Experimental refutation of the deuterium permeability in vanadium, niobium and tantalum. *Fusion Eng. Des.* **2019**, *146*, 224–227. [[CrossRef](#)]
6. Garcinuño, B.; Rapisarda, D.; Fernández-Berceruelo, I.; Carella, E.; Sanz, J. The CIEMAT LiPb Loop Permeation Experiment. *Fusion Eng. Des.* **2019**, *146*, 1228–1232. [[CrossRef](#)]
7. Taylor, C.N.; Fuerst, T.F.; Pawelko, R.J.; Shimada, M. The Tritium Extraction eXperiment (TEX): A forced convection fusion blanket PbLi loop. *Fusion Eng. Des.* **2023**, *192*, 113737. [[CrossRef](#)]
8. Papa, F.; Utili, M.; Venturini, A.; Caruso, G.; Savoldi, L.; Bonifetto, R.; Valerio, D.; Allio, A.; Collaku, A.; Tarantino, M. Engineering design of a Permeator against Vacuum mock-up with niobium membrane. *Fusion Eng. Des.* **2021**, *166*, 112313. [[CrossRef](#)]
9. Venturini, A.; Papa, F.; Utili, M.; Forgione, N. Experimental Qualification of New Instrumentation for Lead-Lithium Eutectic in IELLLO Facility. *Fusion Eng. Des.* **2020**, *156*, 111683. [[CrossRef](#)]
10. Utili, M.; Alberghi, C.; Candido, L.; Papa, F.; Tarantino, M.; Venturini, A. TRIEX-II: An experimental facility for the characterization of the tritium extraction unit of the WCLL blanket of ITER and DEMO fusion reactors. *Nucl. Fusion* **2022**, *62*, 066036. [[CrossRef](#)]
11. Tarantino, M.; Martelli, D.; Del Nevo, A.; Utili, M.; Di Piazza, I.; Eboli, M.; Diamanti, D.; Tincani, A.; Miccichè, G.; Bernardi, D.; et al. Fusion technologies development at ENEA Brasimone Research Centre: Status and perspectives. *Fusion Eng. Des.* **2020**, *160*, 112008. [[CrossRef](#)]
12. Utili, M.; Alberghi, C.; Bonifetto, R.; Candido, L.; Collaku, A.; Garcinuño, B.; Kordac, M.; Martelli, D.; Mozzillo, R.; Papa, F.; et al. Design and integration of the WCLL Tritium Extraction and Removal System into the European DEMO tokamak Reactor. *Energies* **2023**, *16*, 5231. [[CrossRef](#)]
13. Pressure Equipment Directive 2014/68/EU. Available online: <https://osha.europa.eu/en/legislation/directive/directive-201468-eu-pressure-equipment> (accessed on 26 June 2023).
14. ISO 18279; Brazing—Imperfections in Brazed Joints. ISO: Geneva, Switzerland, 2003.
15. Feuerstein, H.; Gräbner, H.; Oschinski, J.; Horn, S. Compatibility of refractory metals and beryllium with molten Pb-17Li. *J. Nucl. Mater.* **1996**, *233*, 1383–1386. [[CrossRef](#)]
16. Gräbner, H.; Feuerstein, H.; Oschinski, J. Compatibility of metals and alloys in liquid Pb-17Li at temperatures up to 650 °C. *J. Nucl. Mater.* **1988**, *155*, 702–704. [[CrossRef](#)]
17. Venturini, A.; Bassini, S.; Ciantelli, C.; Fiore, A.; Martelli, D.; Papa, F.; Utili, M. Compatibility of niobium, vanadium and P22 steel in high temperature flowing LiPb. *J. Nucl. Mater.* **2022**, *571*, 153985. [[CrossRef](#)]
18. Mathon, M.; Connétable, D.; Sundman, B.; Lacaze, J. CALPHAD-type assessment of the Fe-Nb-Ni ternary system. *Comput. Coupling Phase Diagr. Thermochem.* **2009**, *33*, 136–161. [[CrossRef](#)]

Disclaimer/Publisher’s Note: The statements, opinions and data contained in all publications are solely those of the individual author(s) and contributor(s) and not of MDPI and/or the editor(s). MDPI and/or the editor(s) disclaim responsibility for any injury to people or property resulting from any ideas, methods, instructions or products referred to in the content.